

# Surface intercalation of gold underneath a graphite monolayer on Ni(111) studied by angle-resolved photoemission and high-resolution electron-energy-loss spectroscopy

A. M. Shikin, G. V. Prudnikova, and V. K. Adamchuk

*Institute of Physics, St. Petersburg State University, St. Petersburg, 198904, Russia*

F. Moresco and K.-H. Rieder

*Fachbereich Physik, Freie Universität Berlin, D-14195, Berlin, Germany*

(Received 20 April 2000)

Quasi-two-dimensional intercalationlike systems, synthesized by surface intercalation of gold atoms underneath a monolayer of graphite formed on Ni(111), have been investigated by angle-resolved photoemission spectroscopy (PES) and high-resolution electron-energy-loss spectroscopy (HREELS). Modifications of both electronic structure and vibrational properties due to the presence of the intercalated Au monolayer between the graphite monolayer and Ni(111) are reported. The surface intercalation of the gold atoms underneath the graphite monolayer leads to a “stiffening” of the graphite-derived phonon modes and to an energetic shift of the graphite-derived  $\pi$ ,  $\sigma$  electronic states in the valence band toward lower binding energies. The observed changes of the PE and HREEL spectra are explained by the saturation of the active Ni( $d$ ) bonds by the intercalated gold atoms and by the weakening of the interaction between graphite monolayer and substrate, due to the blockage of the graphite C( $\pi$ )-Ni( $d$ ) hybrid bonds.

## INTRODUCTION

The mechanism of formation and the electronic and crystalline structure of surface quasi-two-dimensional intercalationlike systems, synthesized from a monolayer of graphite formed on Ni(111) by cracking of carbon-containing gases and by surface intercalation of different metals underneath it, has been studied in recent years.<sup>1-9</sup> These systems are characterized by a close fit between the lattice parameters of the graphite monolayer and those of the Ni(111) substrate,<sup>10-12</sup> which allows formation of well-ordered commensurate quasi-low-dimensional layered structures. Among the metals that can be intercalated underneath a monolayer of graphite, noble metals (Au, Ag, Cu) now attract enhanced interest because under normal conditions they cannot form graphite intercalation compounds (GIC's) of bulk type.<sup>13</sup> The ability to form quasi-two-dimensional intercalationlike systems on Ni(111) by the surface intercalation of noble metals underneath a graphite monolayer therefore gives a unique possibility to study the characteristics of such systems and to investigate the mechanism of their formation.

Some recent investigations show that important physical properties characterize such systems. In particular, in Ref. 14 the “semiconductor-metal” transition observed in plasma-sputtered C-Cu films as a function of copper concentration is connected to the formation of clusters of Cu-derived GIC's in the bulk, and in Ref. 15 the high- $T_c$  superconductivity of such systems is discussed. Another interesting aspect of the surface intercalation of noble metal underneath a monolayer of graphite (MG) is the “stiffening” of the phonon modes that has been revealed, for instance, for MG/Cu/Ni(111) and MG/Ag/Ni(111).<sup>1-4</sup> Such an effect has not been observed up to now for any other system of intercalationlike type.<sup>13,16</sup>

While our earlier works<sup>1-4</sup> were mainly devoted to studying the intercalation of copper and silver underneath a graphite monolayer on Ni(111) by means of high-resolution

electron-energy-loss spectroscopy (HREELS), in the present investigation we have studied the processes of intercalation of gold (with different thicknesses of the preliminary deposited overlayer) underneath a graphite monolayer formed on Ni(111). In particular, we have exploited the modifications of the electronic structure of the valence band and of the phonon spectra caused by this intercalation. The experiment was performed by a combination of angle-resolved HREELS with angle-resolved photoelectron spectroscopy (PES). As reported in Refs. 1-5, the analysis of the intercalation process was based on the modification of the energy and intensity of the graphite-derived  $\pi$ ,  $\sigma$  states in PES upon annealing of the system<sup>5</sup> and on the observation of graphitelike structure in the phonon spectra, which are very sensitive to the presence and chemical state of carbon at the surface (see, for instance, Refs. 17 and 18) and can therefore indicate the termination of a system with a graphite overlayer.<sup>1-4</sup>

We show in the present paper that the intercalation of a thin Au layer underneath a graphite monolayer, which takes place upon thermal annealing of the MG/Ni(111) system after deposition of a thin gold overlayer (3-9 Å), causes a “stiffening” of the graphite-derived phonon modes and an energetic shift of the graphite-derived  $\pi$ ,  $\sigma$  valence bands toward lower binding energies, to the values characteristic for bulk monocrystalline graphite. In contrast, the deposition of a thick gold overlayer (60 Å) on MG/Ni(111) followed by annealing does not lead to the formation of an intercalationlike system terminated by a graphite monolayer. The observed changes of the HREEL and PE spectra after intercalation are explained by blocking of the MG( $\pi$ )-Ni( $d$ ) interaction due to the penetration of gold atoms into the space between the graphite monolayer and the Ni substrate.

## EXPERIMENTAL DETAILS

The experiments were performed in two separate ultrahigh-vacuum (UHV) chambers with basic pressure

lower than  $1 \times 10^{-10}$  mbar, equipped with low-energy electron diffraction (LEED), ion gun, and gas inlet systems. The angle-resolved HREEL spectra were measured by means of an ELS22 HREEL spectrometer consisting of two double-cylindrical  $127^\circ$  deflectors. The energy resolution of the spectrometer was 6–8 meV at a primary electron energy of 18.2 eV. This primary electron energy was chosen to provide a parallel transferred momentum high enough to reach the Brillouin zone boundary. The incidence angle of the electron beam was either  $75^\circ$  or  $60^\circ$ , as measured from the direction normal to the surface. The scattering geometry has been chosen to coincide with the  $\Gamma M$  direction of the Ni(111) surface. Angle-resolved photoemission measurements were carried out with an ARIES spectrometer at the Berliner Elektronenspeicherring für Synchrotronstrahlung (BESSY-I, beamline TGM-3) using monochromatic light with a photon energy of 50 eV.

The Ni(111) single crystal was prepared in UHV by several cycles of  $\text{Ne}^+$  sputtering and by high-temperature treatments in oxygen and hydrogen.<sup>10</sup> The graphite monolayer was formed on the Ni(111) surface by cracking propylene ( $\text{C}_3\text{H}_6$ ) at a sample temperature ( $T$ ) of  $500^\circ\text{C}$  as reported in Refs. 1–6. The sample was exposed to a pressure of  $1 \times 10^{-6}$  mbar for 4–5 min to form a graphite monolayer and to saturate the Ni(111) surface. The corresponding LEED pattern displayed the sharp hexagonal structure that characterizes monocrystalline graphite.

Overlayers of gold of different thicknesses (4, 9, and 60 Å) were deposited at room temperature on MG/Ni(111) from gold beads molten on a thin W-Re wire. The thickness of the metal overlayer was monitored with a quartz microbalance. After the deposition of gold, the system showed a diffuse LEED pattern characterized by low-intensity diffraction spots. After annealing at a temperature of  $300\text{--}400^\circ\text{C}$ , the system showed an ordered LEED pattern accompanied by a significant increase of the reflected beam intensity, while phonon modes with graphitelike dispersion appeared in the HREEL spectra. As will be shown later, the annealing of the system allows the intercalation of the gold atoms underneath the graphite monolayer and the restoring of a graphite overlayer on top of the system (at least for the systems with 4 and 9 Å of gold coverage).

## EXPERIMENTAL RESULTS

In Fig. 1 a series of normal-emission photoelectron spectra, corresponding to different thickness of the Au layer (4, 9, and 60 Å) deposited on MG/Ni(111) before and after annealing at  $400^\circ\text{C}$  is shown. The spectrum of a monocrystalline film of Au(111) with a thickness of 20 Å on W(110) and that corresponding to pure MG/Ni(111) are also presented for comparison. As one can see, the spectrum of MG/Ni(111) is characterized by the Ni( $d$ ) states located at binding energy (BE) of 0.5 and 1.5 eV and by the graphite  $\pi_{1v}$  and  $\sigma_{2,3}$  states situated at BE of about 10 and 5 eV, respectively. The nomenclature used in the current paper for the graphite-derived states of  $\pi$  and  $\sigma$  types is normally used for identification of the electronic states in the valence band of pristine graphite (see, for instance, Ref. 13). After deposition of Au ( $\Theta=4$  and 9 Å) the Ni( $d$ ) and graphite  $\pi_{1v}$ ,  $\sigma_{2,3}$  states are significantly weakened without any visible changes in the

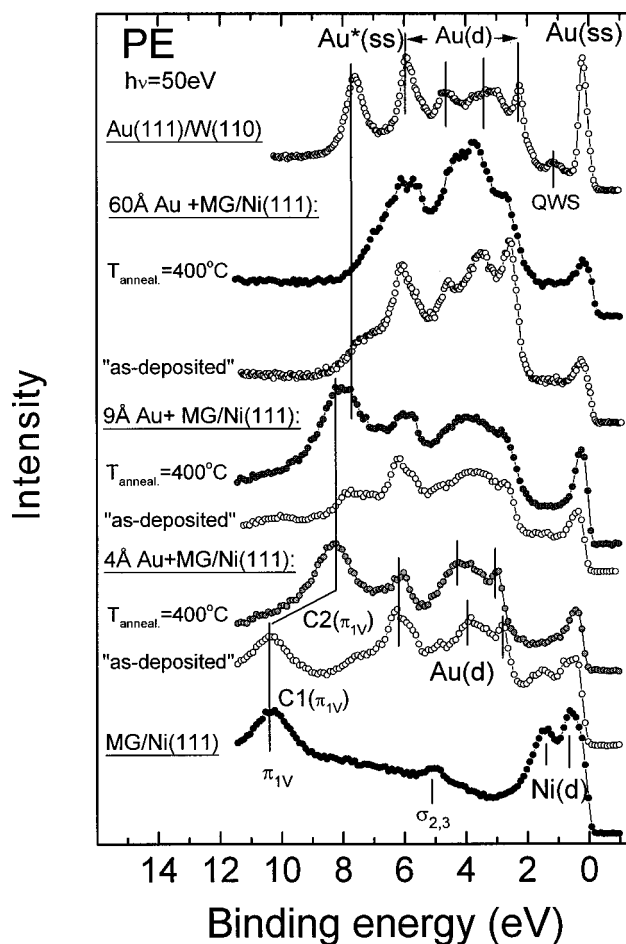


FIG. 1. PE spectra in normal emission upon deposition of gold overlayers of different thickness (4, 9, and 60 Å) on MG/Ni(111) followed by annealing at  $T=400^\circ\text{C}$ . PE spectra for MG/Ni(111) and Au(111)/W(110) are shown for comparison.

BE. The deposition of 9 Å of Au leads to a more significant depletion of the  $\pi_{1v}$  graphite and Ni( $d$ ) states. After deposition of gold, the Au( $d$ ) states located in the region between 2 and 7 eV become dominant. However, in comparison with a monocrystalline Au film on W(110), the spectra of the Au layer deposited on MG/Ni(111) (labeled in Fig. 1 as “as-deposited”) are characterized by a significant depletion of the features related to the Au surface states (for identification of the features in the PE spectrum of gold, see Ref. 19). These peaks are marked in Fig. 1 as Au(ss) and Au\*(ss). In addition, the spectrum of Au(111)/W(110) shows a weak feature related to quantum-well states,<sup>20</sup> which is marked as QWS. The features related to Au surface states are located near the Fermi level ( $E_b \sim 0.35$  eV) and at a BE of 7.7 eV.<sup>19</sup> The QWS are situated at 1.4 eV. For a thickness of 4 Å of the “as-deposited” Au overlayer, the feature near the Fermi level connected with the Au surface states is totally absent in the spectra. The absence of Au surface states and the presence of C( $\pi_{1v}$ ) and Ni( $d$ ) states for the “as-deposited” 4 Å Au overlayer shows the islandlike character of the deposited Au overlayer. The feature near the Fermi level related to the Au surface states is clearly visible only when the gold layer has a thickness of 9 Å, i.e., when the whole surface is covered by gold.

Annealing of the system at  $T \approx 300\text{--}400^\circ\text{C}$  leads to a

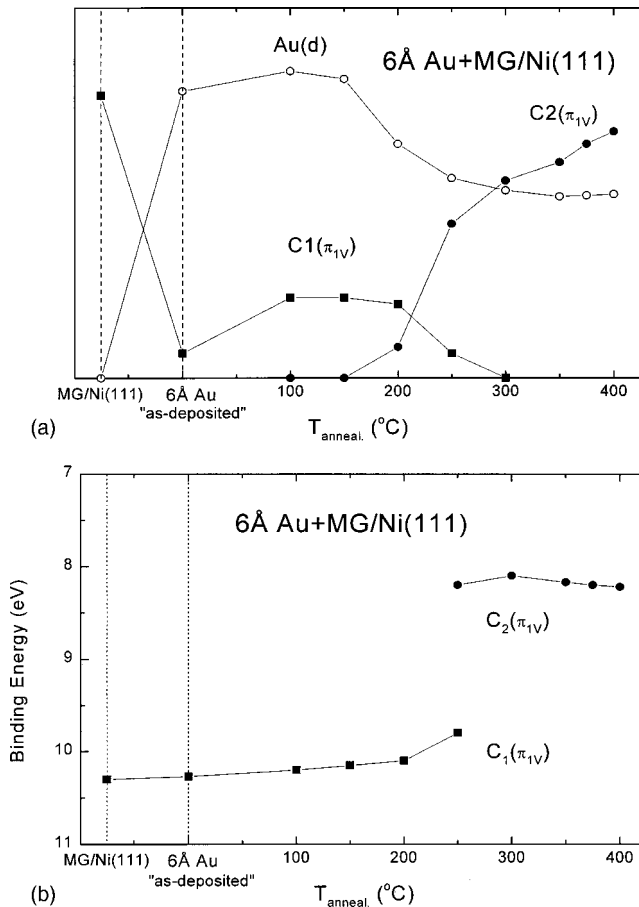


FIG. 2. (a) Variation of the intensity of the unshifted and shifted components of the  $\pi_{1v}$  states at  $E_b \sim 10$  eV [ $C1(\pi_{1v})$ ] and 8 eV [ $C2(\pi_{1v})$ ] and of the Au( $d$ ) states ( $E_b \sim 6$  eV) upon deposition of 6 Å Au on MG/Ni(111) and annealing at different temperatures. (b) Changes of the binding energies of the C1 and C2 components of the  $\pi_{1v}$  states upon annealing at different temperatures.

significant modification of the spectrum. In Fig. 1 the PE spectra after annealing at 400 °C are presented. As one can see, a significant growth of the peak intensity for the  $\pi_{1v}$  graphite states takes place after annealing, accompanied by an energetic shift toward lower binding energies of about 2 eV with respect to Mg/Ni(111), while the Ni( $d$ ) states essentially disappear. The feature near the Fermi level is already visible in PE spectra after annealing and the Au( $d$ ) states are slightly shifted toward higher BE as compared with the “as-deposited” Au overlayer and with the monocrystalline Au film on W(110). The system with a gold overlayer of 9 Å shows a shift of the  $\pi_{1v}$  states slightly higher than that with 4 Å of gold.

The relative peak intensity of the Au( $d$ ) states (located at about 6 eV) is compared in Fig. 2(a) with that of the graphite  $\pi_{1v}$  state characteristic of the initial MG/Ni(111) system ( $E_b \sim 10$  eV), which is marked as C1( $\pi_{1v}$ ), and of the shifted  $\pi_{1v}$  state ( $E_b \sim 8$  eV), which is marked as C2( $\pi_{1v}$ ), observed after the deposition of 6 Å of Au on MG/Ni(111) and after annealing at different temperatures. The variation of the binding energy of the peak of the  $\pi_{1v}$  states [for both C1( $\pi_{1v}$ ) and C2( $\pi_{1v}$ )] upon increase of the annealing temperature is presented in Fig. 2(b). As one can see, after the deposition of gold an intense Au( $d$ ) peak appears in the

spectra, while the intensity of the peak of the  $\pi_{1v}$  states [ $C1(\pi_{1v})$ ] decreases significantly. On the other hand, annealing of the system at 250–300 °C leads to an inversion in the peak intensities: the C2( $\pi_{1v}$ ) peak increases its intensity after annealing at 375–400 °C almost up to the level characteristic of the initial MG/Ni(111) system, while the peak of the Au( $d$ ) states becomes smaller.

The observed variations in the intensity of the PE peaks after annealing, in combination with the significant change of the BE of the graphite  $\pi_{1v}$  states, is related to the penetration of atoms of gold underneath the graphite monolayer and to modification of the interaction of the graphite with the substrate due to surface intercalation. We can therefore conclude that the deposition of thin gold layers (with thicknesses of 4 and 9 Å) on MG/Ni(111) followed by annealing at about 300–400 °C leads to the intercalation of Au atoms underneath the graphite monolayer. It is important to note that, as one can see in Fig. 1, the deposition of thicker Au overlayers ( $\Theta \sim 60$  Å) with subsequent annealing at any temperature does not lead to restoration of the graphite  $\pi_{1v}$  states in the photoemission spectra. Even after annealing, the PE spectra remain similar to those observed for a metallic Au overlayer, showing that a surface intercalationlike compound with a graphite monolayer on top of the system did not form in these conditions.

In Fig. 3 a series of angle-resolved photoemission spectra is presented for the system obtained by deposition of 9 Å of Au on MG/Ni(111) followed by annealing at 400 °C, i.e., after intercalation of gold atoms underneath the graphite monolayer. The spectra are measured for different polar angles in the  $\Gamma M$  direction of the graphite surface Brillouin zone (SBZ) at  $h\nu = 50$  eV. The graphite-derived  $\sigma_1$ ,  $\sigma_{2,3}$ , and  $\pi_{1v}$  states with their characteristic graphitelike dispersion can easily be distinguished in the spectra. The corresponding dispersion relations in the  $\Gamma M$  direction are represented in Fig. 4 by solid circles. Here, for comparison, the dispersion curves of the initial MG/Ni(111) system and of bulk monocrystalline graphite are shown by open circles (solid lines) and open squares (dotted lines), respectively. The curves for monocrystalline graphite were taken from Ref. 21. From analysis of the photoemission spectra presented it is possible to conclude that the graphite-derived states of MG/Au/Ni(111) are shifted toward the Fermi level. This shift is about 2 eV for the  $\pi_{1v}$  states and 0.5–1 eV for the  $\sigma_1$  and  $\sigma_{2,3}$  states. After intercalation of Au the branch of the  $\pi_{1v}$  states essentially coincides with that typical for bulk monocrystalline graphite. At the same time, the  $\sigma_1$  states are located in a region of BE even lower than that characteristic of monocrystalline graphite. The minimum of the BE of the  $\pi_{1v}$  and  $\sigma_1$  states was observed for polar angles of about 26° relative to the surface normal, corresponding, at  $h\nu = 50$  eV, to the  $M$  point of the graphite SBZ.

In Fig. 5 we show a series of angle-resolved HREEL spectra for the system formed by the deposition of 6 Å of Au on MG/Ni(111) followed by annealing at  $T = 400$  °C. The spectra were measured in the  $\Gamma M$  direction of the graphite SBZ for different angles of scattering and show a main graphite-derived phonon mode which can be separated into the vertical acoustic mode ZA, the longitudinal acoustic mode LA, the acoustical shear horizontal mode SH, the vertical optical mode ZO, the optical shear horizontal mode

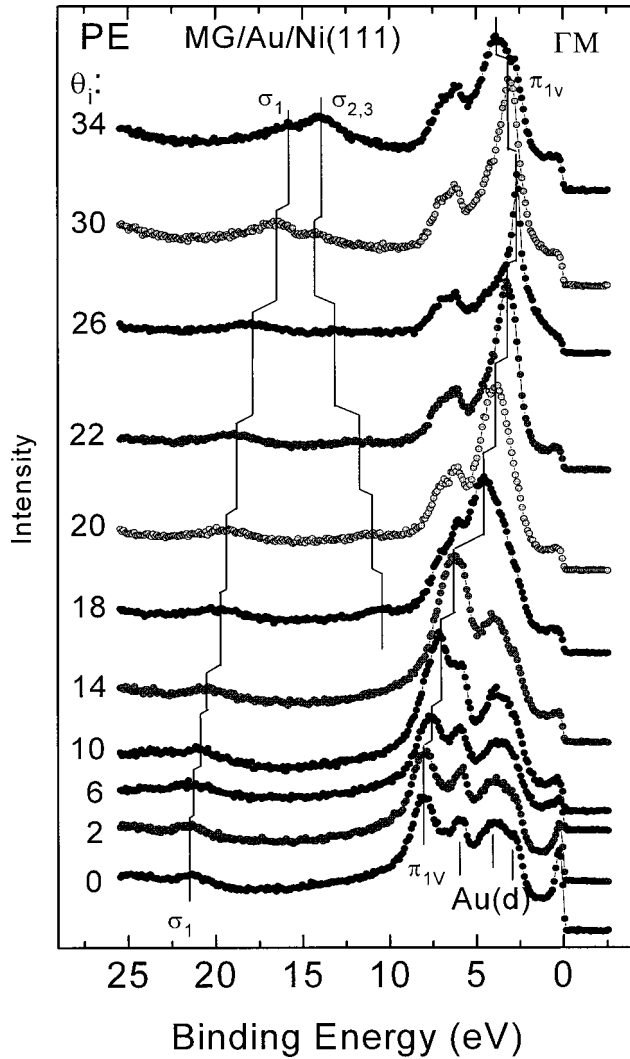


FIG. 3. Angle-resolved PE spectra for MG/Au/Ni(111) formed after deposition of 9 Å of Au on MG/Ni(111) and annealing at 400 °C. The spectra are measured at  $h\nu=50$  eV in the  $\Gamma M$  direction at different polar angles ( $\theta_i$ ) relative to the surface normal.

SH\*, and the longitudinal optical mode LO. All the features are characterized by a pronounced graphitelike dispersion. No other loss peak has been observed in the HREEL spectra, showing that the system formed by annealing terminates with a graphite monolayer and that surface intercalation of Au atoms underneath the graphite monolayer has occurred.

The dispersion relations of the graphite-derived phonon modes measured by HREELS in the  $\Gamma M$  direction are presented in Fig. 6 for different thicknesses (3 and 6 Å) of the Au overlayer. The spectra were measured at incidence angles of 60° and 75° relative to the surface normal (solid symbols). The surface phonon dispersions for MG/Ni(111) and pristine (monocrystalline) graphite are shown by open circles and squares and dotted lines, respectively. The phonon dispersion for pristine graphite was taken from Ref. 22. As one can see in Fig. 6, the surface intercalation of Au atoms underneath a graphite monolayer leads to a noticeable shift of the phonon modes to higher energy losses. Such modes are located essentially at the energies characteristic of the phonon modes of bulk graphite. The maximal energy shift (about 15–20 meV) toward higher energies (the so-called stiffening of the

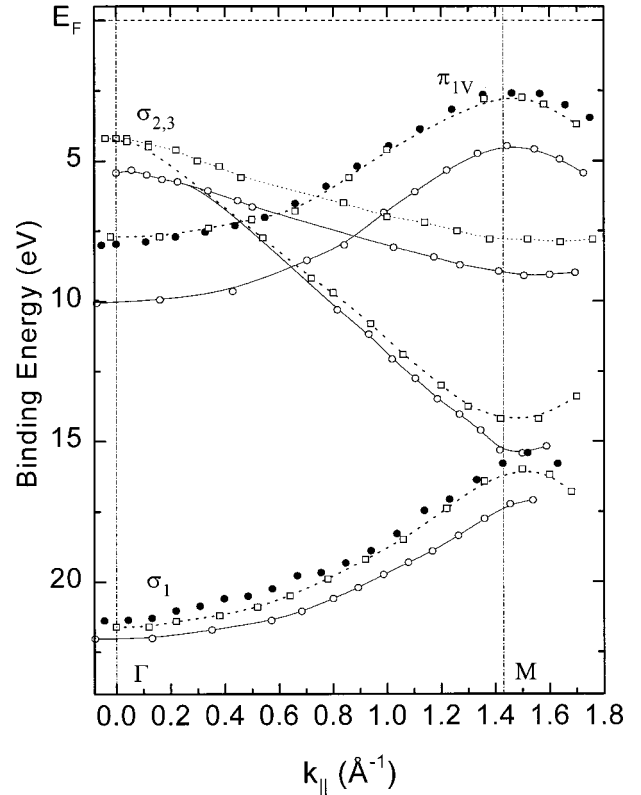


FIG. 4. Dispersion of the main graphite-derived valence band electronic states (solid circles) as obtained from the PE spectra in Fig. 3. The dispersions of MG/Ni(111) (open circles and straight lines) and of bulk monocrystalline graphite (open squares and dotted lines) are shown for comparison.

phonon modes) was observed for the ZO mode connected with the vibrations of the carbon atom perpendicular to the surface. The LA mode does not differ so much from that of bulk graphite and from the mode observed for MG/Ni(111). Since this mode is associated with the vibrations of the carbon atom parallel to the surface (i.e., in the direction of the  $\sigma$  bonds,<sup>22</sup>) we can assign it to the graphite overlayer. For the ZA mode an energetic shift toward higher loss energies was also observed in the region of the  $M$  point, at the edge of the Brillouin zone.

It is important to note that the changes in the phonon branch do not saturate near the  $M$  point of the SBZ, as they extend to transfer momentum ( $q_{\parallel}$ ) bigger than about 1.4 Å<sup>-1</sup>. Such behavior is similar to that observed in the  $\Gamma K$  direction,<sup>1–4</sup> where the edge of the SBZ ( $K$  point) corresponds to  $q_{\parallel}=1.7$  Å<sup>-1</sup> and is probably related to some misorientation of areas (domains) in the graphite monolayer caused by the Au intercalation. It is interesting to note that for MG/Ni(111) the  $M$  point of the SBZ can be seen as the border of the periodic changes of the phonon energy (Fig. 6). Some support for this assumption comes from observation of the optical shear horizontal mode SH in MG/Au/Ni(111), which should be forbidden by the scattering geometry used in the experiment.<sup>23</sup> The presence of this mode might be a consequence of a symmetry-breaking effect caused by modification of the graphite substrate bonding after the Au intercalation. By comparing the MG/Au/Ni(111) case with the MG/Ni(111) system one can observe for both systems an energetic shift and a variation of the (LO+SH\*) mode. More-

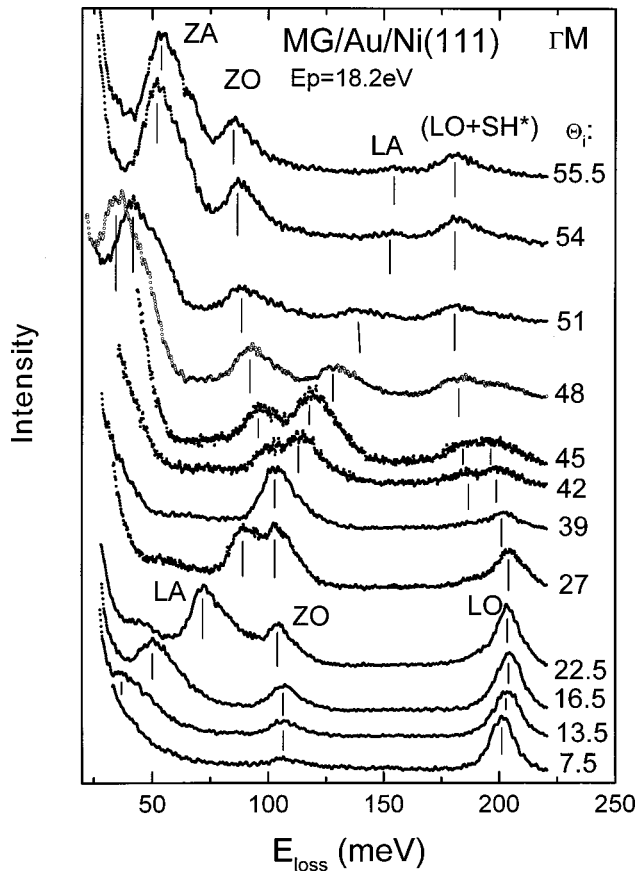


FIG. 5. Angle-resolved HREEL spectra of MG/Ni(111) formed after deposition of 6 Å of Au on MG/Ni(111) and annealing at 400 °C. The spectra are measured in the  $\Gamma M$  direction at different angles of incidence relative to the surface normal: 60° for scattering angles lower than 27° and 75° for scattering angles above 39°.

over, if for MG/Ni(111) the SH\* mode is dominant, for MG/Au/Ni(111) mainly the LO mode was observed.

## DISCUSSION

It is now well established<sup>7,8,22</sup> that the interaction of a graphite monolayer with a Ni(111) substrate causes orbital mixing of the graphite  $\pi$  states with  $d$  states of the Ni substrate. This interaction is covalentlike and leads to an electronic redistribution between the bonding  $\pi$  and antibonding  $\pi^*$  states and to a significant “softening” of the graphite-derived phonon modes in comparison with those of bulk graphite. In the valence band, the hybridization of the graphite  $\pi$  states with the substrate Ni( $d$ ) states causes a shift of the graphite-derived  $\pi$  and  $\sigma$  states toward higher binding energies. As the interaction of the Ni( $d$ ) states of the substrate with the graphite  $\pi$  states is stronger than with the  $\sigma$  states, the binding energies of the  $\sigma$  states are less influenced than those of the graphite  $\pi$  states. The dispersion dependencies in Fig. 4 manifest these effects, where the shift of the  $\pi$  states is about 2 eV, while the  $\sigma$  states of MG/Ni(111) are shifted only by 0.5–1 eV as compared to those of pristine graphite.

The intercalation of gold atoms leads to a modification of the interaction between graphite monolayer and substrate. According to their phase diagrams,<sup>24</sup> gold and carbon are

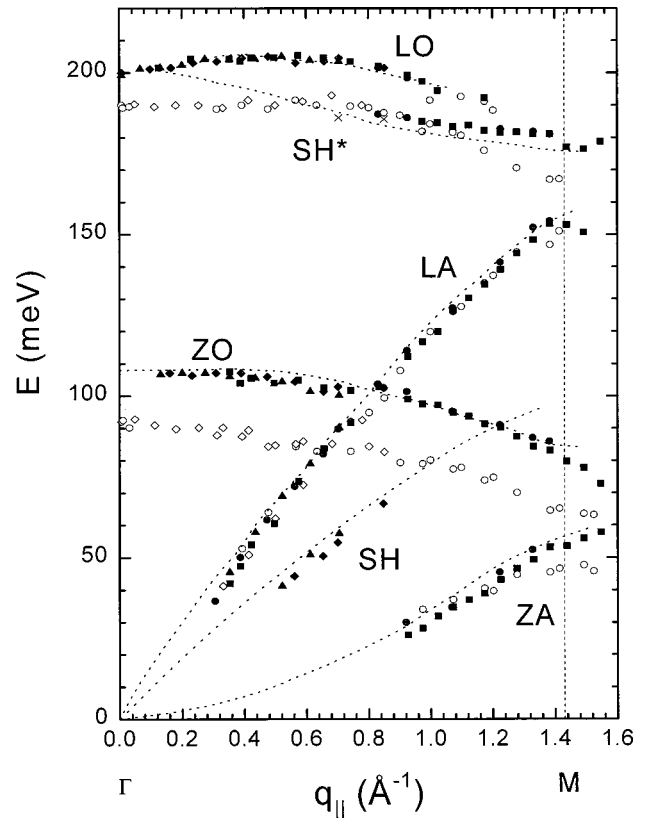


FIG. 6. Dispersion relations of the graphite-derived phonon modes for MG/Ni(111) systems formed after deposition of Au layers of different thicknesses 3 (solid triangles and squares) and 6 Å (solid circles and rhombus) and subsequent annealing at 400 °C. The measurements were performed in the  $\Gamma M$  direction at the angles of incidence 60° (triangles and rhombus) and 75° (circles and squares) relative to the surface normal. The surface phonon dispersions for the MG/Ni(111) system (open symbols) and for bulk monocrystalline graphite taken from Ref. 22 (dotted lines) are also shown.

characterized by a very low mutual chemical activity in normal conditions. On the other hand, the phase diagram of the binary (Ni-Au) system displays good solubility of the different elements and high mutual chemical activity.<sup>24</sup> Therefore one would expect that the intercalation of gold underneath a graphite monolayer would lead to saturation of the active Ni( $d$ ) states and to blockade of the (C)( $\pi$ )-Ni( $d$ ) hybridization, resulting in a weakening of the graphite-monolayer-substrate covalent interaction. As a consequence we expect to observe a reversal of the energetic shift of the graphite-derived electronic states in the valence band and of the phonon modes toward the positions characteristic for pristine graphite, where the interaction between the graphite planes is weak. Such an effect was indeed observed in the present experiment and, in the phonon spectra, it displays itself as a “stiffening” of the ZO, ZA, and LO modes. The ZO and ZA modes are responsible for the vertical vibrations of the carbon atoms (i.e., in the direction of the graphite  $\pi$  bonds). Therefore, the weakening of the graphite-monolayer-substrate interaction, which works mainly via the graphite  $\pi$  bonds, leads to modification of these phonon modes toward the energy characteristic of bulk graphite. The LA mode for MG/Au/Ni(111) is situated in the same region for both bulk

graphite and MG/Ni(111), demonstrating that the top overlayer of the systems is graphite. As one can see from Fig. 6, the effect of “stiffening” of the phonon vibrations is also observed for the LO mode as compared with the initial MG/Ni(111) system. According to Refs. 7, 8, and 22, the energy of this mode is strongly influenced by filling of the graphite  $\pi^*$  antibonding states. In the case of blockade of the C( $\pi$ )-Ni( $d$ ) interaction due to Au intercalation, the additional occupation of the  $\pi^*$  antibonding states, which takes place for MG/Ni(111), is decreased and results in the observed “stiffening” of the LO mode for MG/Au/Ni(111). In addition, after intercalation of Au, the SH mode can be clearly distinguished in the HREEL spectra, probably because of the symmetry-breaking effect<sup>23</sup> introduced by an orientation misfit between the graphite monolayer and the underlying intercalated Au layer. It should be noted that the energetic position of this mode is essentially the same as in the case of bulk graphite.

We can therefore conclude that all the observed modifications in the photoemission and phonon spectra are connected to the penetration of gold atoms into the space between graphite and Ni and can be explained in terms of a significant weakening of the graphite-monolayer–substrate interaction, due to blocking of the C( $\pi$ )-Ni( $d$ ) hybridization after the intercalation. These changes in the spectral structure are similar to those observed upon intercalation of Cu and Ag underneath a graphite monolayer on Ni(111),<sup>1–4</sup> and are typical for all intercalationlike systems based on graphite and noble metals.

We now discuss in more detail the changes of PE spectra observed upon intercalation of gold atoms underneath a monolayer of graphite. As one can see in Fig. 1, the deposition of 4 Å of Au causes depletion of the  $\pi_{1v}$  graphite and Ni( $d$ ) states, while the increase of thickness up to 9 Å leads essentially to the disappearance of these states from the PE spectra. Au( $d$ ) states are present in PE spectra already from the first stages of gold deposition. However, in comparison with Au/W(110), the Au( $d$ ) states upon deposition of Au on MG/Ni(111) are characterized by a slight energy shift toward higher binding energies and by a significant depletion of the features related to the Au surface states located at 8 and 0.4 eV (see Ref. 19 for the assignment of Au surface states). For a 4 Å gold overlayer the feature near the Fermi level related to Au(ss) is essentially absent in the PE spectra. Annealing of both systems (4 and 9 Å of gold) leads to restoration of the  $\pi_{1v}$  states (shifted toward lower BE), to the total disappearance of the Ni( $d$ ) states, and to the appearance of the feature near the Fermi level. We connect these changes of the PE spectra with the transformation of the system from Au islands on top of the MG/Ni(111) surface to a continuously distributed smooth gold interlayer between graphite monolayer and Ni substrate which was formed after gold intercalation. The presence of the Ni( $d$ ) states in the 4 Å case, their disappearance after annealing, and the appearance of the feature near the Fermi level support such assumptions [the weakened surface-derived states at the Fermi level was also observed in Refs. 25 and 26 upon deposition of Fe and benzenethiol monolayers on Cu(111) and Au(111), respectively].

As we noted before, the deposition of 60 Å of gold followed by annealing at  $T = 400^\circ\text{C}$  does not lead to restoration

of the peak of the  $\pi_{1v}$  states in PE spectra. The corresponding PE spectra are characterized by a structure mainly similar to that of a metallic gold film on W(110) with significantly depleted Au surface states. We can then conclude, therefore, that the deposition of a thick gold overlayer on MG/Ni(111) followed by annealing does not lead to the formation of a surface intercalationlike system with a graphite monolayer on top. It is interesting to note that the deposition of thick layers of other noble metals (for instance, Cu) followed by annealing at about  $400^\circ\text{C}$  restores the graphite  $\pi_{1v}$  states, shifted toward lower energies, indicating the formation of well-identified surface-intercalation-like systems.<sup>6</sup> The different behavior of gold can be primarily related to its bigger atomic radius. The maximal amount of intercalated gold seems to be about one monolayer, as supported by the fact that the intensity of the Au( $d$ ) peaks after annealing is similar for gold overlayers with different thickness (4 and 9 Å). For the MG/Cu/Ni(111) system we observed, on the other hand, a strong dependence of the intensity of the Cu( $d$ ) states after intercalation on the thickness of the deposited Cu overlayer.<sup>6</sup> In relation to MG/Au/Ni(111), as the first intercalated gold monolayer saturates all active Ni( $d$ ) states, there is afterwards no additional stimulus for further intercalation of gold. On the other hand, the fact that a graphite monolayer does not segregate to the surface through the thick gold overlayer (it is absent on top of the system with 60 Å of Au) can also be related to the dissolving of graphite in thick (massive) gold during its segregation to the surface. According to the binary phase diagrams,<sup>24</sup> such processes can take place in a bulk Au-C system in the presence of a small carbon concentration.

Furthermore, as one can see from Fig. 1, the observed shift of the  $\pi_{1v}$  states is visibly bigger in the case of 9 Å of gold than in the case of 4 Å. This effect can be related to overlapping with the Au\*(ss) states located at about of 7.7 eV, which is expected to be stronger for a continuous and thicker Au layer. Alternatively, it might be connected to some healing of defects at steps of the Ni(111) surface and to the better saturation of the Ni( $d$ ) states by intercalated gold atoms in the 9 Å case. The gold atoms that are not intercalated can accumulate in the form of islands near these defects. The experimental fact that in the dispersion curves the branch of the  $\sigma_1$  states (Fig. 4) is located slightly above the corresponding branch in bulk graphite can also be explained by assuming that the intercalated gold layer totally saturates the Ni( $d$ ) bonds [and the defects at the Ni(111) surface], significantly weakening the covalent interaction between graphite monolayer and substrate. In this case the properties of the surface graphite monolayer become closer to those typical of a single graphite sheet (i.e., graphene).

## CONCLUSION

By using angle-resolved photoemission and HREELS, we have investigated the process of surface intercalation of gold atoms underneath a graphite monolayer deposited on the Ni(111) surface and the modifications induced by such intercalation in the electronic and vibrational structure. We have shown that intercalation takes place when a thin layer of gold (3–9 Å) is deposited on MG/Ni(111) and then annealed at  $T = 350\text{--}400^\circ\text{C}$ . The deposition of thicker gold overlayers

( $\sim 60$  Å) with subsequent annealing does not lead to the expected termination of the system by a graphite overlayer on to the formation of a surface-intercalation-like system. Analysis of the measured spectra allows us to conclude that only about one monolayer from the 3–9 Å thick Au overlayer deposited can be inculcated between a monolayer of graphite and the Ni(111) surface. The gold atoms not intercalated accumulate on the surface in the form of islands. We have also shown that the intercalation of gold underneath a graphite monolayer causes a “stiffening” of the graphite-derived phonon modes as observed in the HREEL spectra and a shift of the graphite electronic states in the valence band toward lower binding energies, to the typical values observed for bulk monocrystalline graphite. The observed modifications of the HREEL and PE spectra can be explained by saturation of the active Ni(*d*) bonds and by

blocking of the MG-Ni interaction due to the intercalation of the gold atoms in the space between the graphite sheet and the Ni(111) surface. As a consequence the electronic and vibrational properties of the topmost graphite layer become similar to those of bulk graphite.

#### ACKNOWLEDGMENTS

This work was supported by the Deutsche Forschungsgemeinschaft, by the programs “Surface atomic structure” and “Fullerenes and atomic clusters,” and by the RFFI-DFG Program (Project No. 98-03-04071). A.M.Sh. is grateful to the Freie Universität Berlin for financial support and hospitality. The authors thank Christian Roth for technical assistance.

- 
- <sup>1</sup>A. M. Shikin, D. Farias, and K.-H. Rieder, *Europhys. Lett.* **44**, 44 (1998).
- <sup>2</sup>A. M. Shikin, D. Farias, V. K. Adamchuk, and K.-H. Rieder, *Surf. Sci.* **424**, 155 (1999).
- <sup>3</sup>D. Farias, A. M. Shikin, K.-H. Rieder, and Yu. S. Dedkov, *J. Phys.: Condens. Matter* **11**, 8453 (1999).
- <sup>4</sup>D. Farias, K.-H. Rieder, A. M. Shikin, V. K. Adamchuk, T. Tanaka, and C. Oshima, *Surf. Sci.* **454-456**, 437 (2000).
- <sup>5</sup>A. M. Shikin, M. V. Poygin, Yu. S. Dedkov, S. L. Molodtsov, and V. K. Adamchuk, *Fiz. Tverd. Tela (St. Petersburg)* **42**, 173 (2000) [*Phys. Solid State* **42**, 173 (2000)].
- <sup>6</sup>Yu. S. Dedkov, A. M. Shikin, V. K. Adamchuk, S. L. Molodtsov, C. Laubschat, A. Bauer, and G. Kaindl (unpublished).
- <sup>7</sup>A. Nagashima, N. Tejima, and C. Oshima, *Phys. Rev. B* **50**, 17 487 (1994).
- <sup>8</sup>C. Oshima and A. Nagashima, *J. Phys.: Condens. Matter* **9**, 1 (1997).
- <sup>9</sup>A. Ya. Tontegode, *Prog. Surf. Sci.* **38**, 201 (1974).
- <sup>10</sup>J. C. Shelton, H. R. Patil, and J. M. Blakely, *Surf. Sci.* **43**, 493 (1974).
- <sup>11</sup>T. Aizawa, R. Souda, Y. Ishizawa, H. Hirano, T. Yamada, and K. Tanaka, *Surf. Sci.* **237**, 194 (1990).
- <sup>12</sup>Y. Gamo, A. Nagaschina, M. Wakabayashi, M. Terai, and S. Oshima, *Surf. Sci.* **374**, 61 (1997).
- <sup>13</sup>M. S. Dresselhaus and G. Dresselhaus, *Adv. Phys.* **30**, 139 (1981).
- <sup>14</sup>V. I. Vvanov-Omskii, M. I. Abaev, and S. G. Yastrebov, *Pis'ma Zh. Tekh. Fiz.* **20**, 61 (1994) [*Tech. Phys. Lett.* **20**, 917 (1994)].
- <sup>15</sup>N. E. Bazieva, S. G. Yastrebov, V. K. Masterov, and O. V. Prihodko, *Mol. Mater.* **4**, 143 (1994).
- <sup>16</sup>H. Zabel and S. A. Solin, *Graphite Intercalation Compounds* (Springer, New York, 1998).
- <sup>17</sup>A. M. Shikin, V. K. Adamchuk, S. Siebentritt, K.-H. Rieder, S. L. Molodtsov, and C. Laubschat, *Phys. Rev. B* **61**, 7752 (2000).
- <sup>18</sup>S. Siebentritt, R. Pues, K.-H. Rieder, and A. M. Shikin, *Phys. Rev. B* **55**, 7927 (1997).
- <sup>19</sup>S. D. Kevan and R. H. Gaylord, *Phys. Rev. B* **36**, 5809 (1987).
- <sup>20</sup>A. M. Shikin, D. V. Vyalikh, Yu. S. Dedkov, G. V. Prudnikova, V. K. Adamchuk, E. Weschke, and G. Kaindl, *Phys. Rev. B* **62**, R2303 (2000).
- <sup>21</sup>A. M. Shikin, S. L. Molodtsov, A. G. Vyatkin, V. K. Adamchuk, N. Franco, M. Martin, and M. S. Asensio, *Surf. Sci.* **429**, 287 (1999).
- <sup>22</sup>T. Aizawa, R. Souda, Y. Ishizawa, H. Hirano, T. Yamada, K. Tanaka, and C. Oshima, *Surf. Sci.* **237**, 194 (1990).
- <sup>23</sup>J. P. Toennies, *Surface Phonons*, Vol. 21 of *Springer Series in Surface Science*, edited by W. Kress and F. W. de Wette (Springer, Berlin, 1991).
- <sup>24</sup>*Binary Alloy Phase Diagrams*, edited by T. B. Massalki (ASM International, Materials Park, Ohio, 1990).
- <sup>25</sup>Y. Dong, H. Qian, W. Ren, I. Krash, F. Liu, G. Meng, Z. Lin, and S. Wu, *Solid State Commun.* **108**, 111 (1998).
- <sup>26</sup>C. M. Whelan, C. J. Barnes, Ch. G. H. Walker, and N. M. D. Brown, *Surf. Sci.* **425**, 195 (1999).